*Microsc. Microanal. Microstruct.* **3** (1992) 483–499 DECEMBER **1992**, PAGE 483

Classification
*Physics Abstracts*
73.60B — 73.60 — 78.60H

# Microscale characterisation of epitaxial semiconducting homolayers.
# I. Cathodoluminescence

Christian de Meerschman([1]), Brigitte Sieber([1]), Jean-Louis Farvacque([1]) and Yves Druelle([2])

([1]) Laboratoire de Structure et Propriétés de l'Etat Solide, Unité de Recherche Associée au CNRS n° 234. Bâtiment C6, Université des Sciences et Technologies de Lille, 59655 Villeneuve d'Ascq cedex, France
([2]) IEMN, Université des Sciences et Technologies de Lille, 59655 Villeneuve d'Ascq cedex, France

*(Received 9 July 1992, accepted 3 February 1993)*

**Résumé.** — Nous avons developpé un modèle décrivant la variation de l'intensité de cathodoluminescence (CL) avec la tension d'accélération des électrons incidents. Nous avons étudié spécifiquement le cas d'homostructures semblables à celles utilisées dans la fabrication des transistors à effet de champ. La première couche, de type n, est évaporée sur une couche tampon $\left([N_A] \simeq 10^{15}\ \mathrm{cm}^{-3}\right)$ ; le substrat est semi-isolant. Nous décrivons l'influence des divers paramètres sur les courbes d'intensité CL. Les vitesses de recombinaison à la surface et aux interfaces, ainsi que la longueur de diffusion des porteurs minoritaires peuvent être déterminés à l'échelle du micron$^3$. Nous proposons comme illustration de cette méthode, la caractérisation, dans un microscope électronique à balayage, d'homojonctions d'arséniure de gallium préparées par la technique de jet moléculaire. La couche supérieure est dans un cas dopée avec $4 \times 10^{17}/\mathrm{cm}^3$ atomes de silicium, et dans l'autre avec $2 \times 10^{18}/\mathrm{cm}^3$. Les expériences sont réalisées à température ambiante. La longueur de diffusion diminue d'environ 1 $\mu$m à 0,5 $\mu$m lorsque le niveau de dopage augmente, et les vitesses de recombinaison à la surface et aux interfaces sont de l'ordre de $10^6$ cm/s.

**Abstract.** — A model of the cathodoluminescence (CL) intensity originated from Gallium Arsenide epitaxial layers is developed. The dependence of the CL intensity on the electron beam voltage is investigated in the particular case of a structure which resembles field effect transistors: an n type uppermost layer grown on a acceptor doped $\left([N_A] \simeq 10^{15}\ \mathrm{cm}^{-3}\right)$ layer, the substrate being semi-insulating. The influence of the parameters on which the CL intensity depends is detailed. The surface and interface recombination velocities and the minority carrier diffusion length can be determined in regions of the order of one micron$^3$. As an illustration of the proposed method of characterisation, experiments were performed at room temperature, in a scanning electron microscope, on GaAs homojunctions grown by molecular epitaxy with an uppermost layer silicon doping level of $4 \times 10^{17}$ and $2 \times 10^{18}\ \mathrm{cm}^{-3}$. The minority carrier diffusion length is found to decrease from about 1 $\mu$m to 0.5 $\mu$m when increasing the doping level. The surface and interfaces recombination velocities are estimated to be as high as $10^6$ cm/s.

## 1. Introduction.

The determination of the minority carrier diffusion length ($L$) in semiconductors has been already the subject of a great number of experimental as well as theoretical investigations. The cathodoluminescence (CL) and particularly the electron beam induced current (EBIC) modes of the scanning electron microscope (SEM) have been often preferred to other techniques as a result of their good spatial resolution: this is of great interest when inhomogeneities are present in the material. Numerous reliable EBIC models are available for measuring the diffusion length in bulk specimens, whatever is the junction position with respect to the surface bombarded by the incident electron beam (see for instance [1]). The number of papers dealing with the determination of $L$ in bulk specimens by CL experiments is more limited [2-4]; as a matter of fact, the recent developement of CL comes from the increased interest in optoelectronics semiconductors such as III-V and II-VI compounds. It has the advantage, over EBIC, not to require the preparation of an electrical barrier.

At present, in laser and field effect transistor (FET) technologies, the bulk is only used as a substrate on which are grown thin epilayers. Therefore, a CL model which could be applied to this kind of configuration would allow a local characterisation of the parameters which influence the properties of the devices such as the diffusion length, the absorption coefficient, the surface and interfaces recombination velocities. Similar models have been already developed [5, 6], but none of them applies to the structure we have studied. In fact, each structure has to be modelled in a specific way, and one has to check carefully, before using the results provided by one model, that it is well suited for the structure studied.

In this paper, we report on a CL model for the characterisation of epitaxial homolayers. The calculation is applied to the case where two epilayers are grown on a substrate; this geometry is representative of a FET. More details will be given in section 2.2. The electron beam is perpendicular to the specimen surface and interfaces. The variation of the integral CL signal, modelled as a function of the electron beam voltage, allows the determination of the minority carrier diffusion length and of the surface and interfaces recombination velocities. The method have been applied to the characterisation of GaAs Fets; the homojunctions have been grown by molecular beam epitaxy.

## 2. Model.

2.1 CATHODOLUMINESCENCE INTENSITY OF THE GaAs FET STRUCTURE — Generally speaking, the CL signal coming out of an homogeneous specimen bombarded by an electron beam is:

$$I_{\mathrm{CL}} = \int_V A\,(z)\frac{\Delta p\,(\mathbf{r})}{\tau_{\mathrm{r}}}\,\mathrm{d}^3 r \tag{1}$$

where $V$ is the volume of the specimen, $\tau_{\mathrm{r}}$ the minority carrier radiative lifetime and $\Delta p(\mathbf{r})$ the excess minority carrier density. $A(z)$ is a function which takes into account optical losses [2]:

$$A\,(z) = \int_0^{\vartheta_{\mathrm{c}}} \exp\left(-\frac{\alpha\, z}{\cos\vartheta}\right)\sin\vartheta\,\mathrm{d}\vartheta \tag{2}$$

$\vartheta_{\mathrm{c}}$ is the critical refraction angle at the free surface and $\alpha$ the absorption coefficient. $A(z)$ can be analytically expressed in terms of the exponential integral of the second kind [2].

The CL intensity of an homostructure is given by:

$$I_{CL} = \sum_i \int_{e_{i-1}}^{e_i} A(z) \frac{\Delta p_i(\mathbf{r})}{\tau_{r_i}} d^3r \tag{3}$$

$e_i$ refers to the depth coordinate of the $i^{st}$ interface which lies at the boundary between the $i^{st}$ layer and the $(i+1)^{st}$ layer.

The geometry we have investigated is represented in figure 1. The electron beam is parallel to the $z$ axis; the origin is at the free surface. The minority carrier density in the $i^{st}$ layer $(e_{i-1} < z < e_i)$ is named $\Delta p_i(\mathbf{r})$.

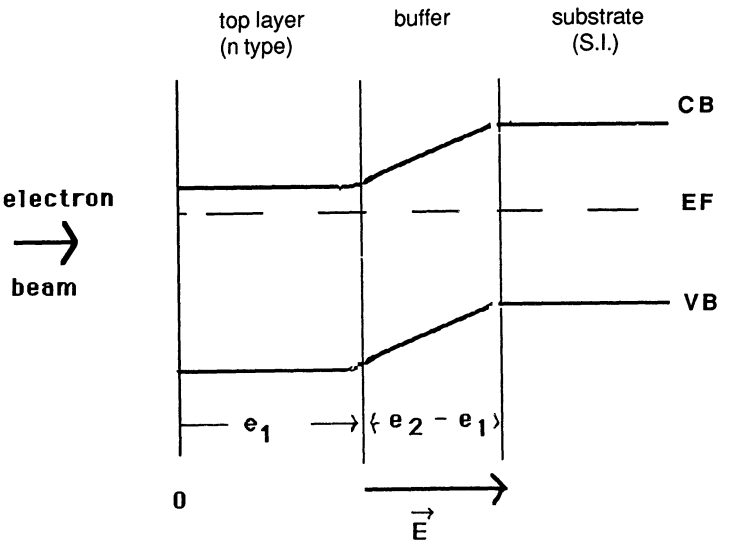


Fig. 1. — Configuration of the homojunction. The electron beam is perpendicular to the surface. The buffer layer, which is non intentionnally doped $\left(N_A = 10^{15}/cm^3\right)$, is between a n type layer $\left(n > 10^{17}/cm^3\right)$ and a semi-insulating substrate. Therefore, it can be considered as depleted of free carriers.

The silicon doping level of the GaAs uppermost layer of the structure ranges from $10^{17}$ to $2 \times 10^{18}$ cm$^{-3}$. The second layer, which is 1 $\mu$m thick, is an non-intentionnally doped layer (the residual acceptor concentration is close to $10^{15}$ cm$^{-3}$) grown on a 350 $\mu$m semi-insulating GaAs substrate. The energy band diagram of this particular configuration is drawn in figure 1. The second layer $(e_1 < z < e_2)$ is a depleted zone due to the differences in the conduction type and doping level of layers 1 and 3, and also because its thickness is quite small. Thus, we can make the assumption that the electrical field within the second layer prevents any radiative recombination, and that the CL signal comes only from the first layer $(0 < z < e_1)$ since its doping level is very high compared to that of the substrate (semi-insulating).

The radiative lifetime $\tau_{r_i}$ is proportional to the inverse of the doping impurity density $N_{d_i}$. This gives for the CL intensity of the structure:

$$I_{CL} \propto N_{d_1} \int_0^{e_1} A(z)\, \Delta p_1(z)\, dz \tag{4}$$

Band bending due to the presence of the free surface separates electron-hole pairs which cumulate in this region. Pseudo Fermi levels are established at equilibrium, and this favours a flattening of the bands if the excess minority carriers cannot be eliminated in a fast enough way. We make in the following the assumption of flat bands conditions in the uppermost layer; this results from the injection level of the CL experiments, from the absence of metal-semiconductor contact, and from the finite thickness of this layer.

2.2 HOLE DENSITIES — In layer $i$, the hole density $\Delta p_i(\mathbf{r})$ satisfies the steady-state continuity equation:

$$\operatorname{div} \mathbf{j}_i = g(\mathbf{r}) - \frac{\Delta p_i(\mathbf{r})}{\tau_i} \tag{5}$$

where $\mathbf{j}_i$ is the hole current density, $\tau_i$ the carrier lifetime, and $g(\mathbf{r})$ the electron-hole pair generation function.

In the first layer, which is n type, the electron beam does not change, under low injection conditions, the electron carrier density. Therefore, the processes of diffusion and recombination only concern the excess holes. The current density $j_1$ at depth $z$ is given by:

$$j_1(z) = -D_1 \left.\frac{\mathrm{d}\,\Delta p_1(z)}{\mathrm{d}z}\right|_z \tag{6}$$

In the case of an homogeneous layer, the hole density satisfies the one-dimensional equation:

$$D_1 \frac{\mathrm{d}^2 \Delta p_1(z)}{\mathrm{d}z^2} - \frac{\Delta p_1(z)}{\tau_1} = -g\,(z) \tag{7}$$

where $g(z)$ is the so-called depth-dose function.

The general solution $\Delta p_1(z)$ has the form:

$$\Delta p_1(z) = A_1 \exp\,(z/L_1) + B_1 \exp\,(-z/L_1) + \int_0^{e_1} \chi_1(z,\, z') \frac{g\,(z')}{D_1}\,\mathrm{d}z' \tag{8}$$

where $\chi_1(z,\, z')$ is the Green function of (7), given by:

$$\chi_1(z,\, z') = \frac{L_1}{2D_1} \exp\left(-\frac{|z - z'|}{L_1}\right) \tag{9}$$

In the second – depleted – layer, the holes are drifted by the electrical field. Therefore we make the assumption that no diffusion and no recombination occur in that region. Consequently, the current density is only a function of the electrical field $E(z)$ :

$$j_2(z) = \mu\, E(z)\, \Delta p_2(z) \tag{10}$$

and we can write equation (5) as:

$$\int\int_S \mathbf{j}_2\,\mathrm{d}\mathbf{S} = \int\int\int_V \mathrm{g}(\mathbf{r})\,\mathrm{d}^3\mathbf{r} \tag{11}$$

In the third semi-insulating layer, where the thermal carrier densities of both types are negligible, the population of electrons and holes which result from the electron beam interaction are

nearly equal. The substrate is therefore subjected to a coupled diffusion of both types of carriers. In such an ambipolar regime, the electron density $\Delta n_3(\mathbf{r})$ and the hole density $\Delta p_3(\mathbf{r})$ satisfy a diffusion-like equation similar to equation (7), but where the diffusion coefficient has to be taken as the ambipolar diffusion coefficient $D_3$ given by:

$$D_3 = \frac{2\, D_{p_3}\, D_{n_3}}{D_{p_3} + D_{n_3}} \tag{12}$$

$D_{p_3}$ and $D_{n_3}$ are the hole and electron diffusion coefficients respectively. Since $D_{n_3}$ is always larger than $D_{p_3}$, $D_3$ is equal to $2D_{p_3}$. Similarly to $j_1$, the expression of the current density $j_3$ at depth $z$ is:

$$j_3(z) = -D_3 \left.\frac{\mathrm{d}\,\Delta p_3(z)}{\mathrm{d}z}\right|_z \tag{13}$$

and $\Delta p_3(z)$ has a form similar to that of $\Delta p_1(z)$ :

$$\Delta p_3(z) = A_3 \exp\,(z/L_3) + B_3 \exp\,(-z/L_3) + \int_{e_2}^{\infty} \chi_3(z, z') \frac{g\,(z')}{D_3} dz' \tag{14}$$

with $\chi_3(z,\ z')$ given by:

$$\chi_3(z,\ z') = \frac{L_3}{2D_3} \exp\left(-\frac{|z - z'|}{L_3}\right) \tag{15}$$

**2.3** BOUNDARY CONDITIONS. — The constants $A_1$, $B_1$, $A_3$ and $B_3$ entering the expression of the hole densities $\Delta p_1(z)$ and $\Delta p_3(z)$ (Eqs. (8) and (14)) are determined from the boundary conditions which are established as follows.

*free surface (z=0):* The excess minority carriers in the uppermost layer can recombine at the free surface, with a recombination rate $V_0$. The minority carrier current density is related to the minority carrier density by:

$$D_1 \frac{\mathrm{d}\,\Delta p_1(z)}{\mathrm{d}z} = V_0\, \Delta p_1(z) \tag{16}$$

*interface 1 ($z = e_1$):* $\mathbf{j}_1(e_1)$ and $\mathbf{j}_2(e_1)$ are the hole current densities in layers 1 and 2 respectively at interface 1. They are related to the interface minority carrier density by:

$$\mathbf{j}_1(e_1) - \mathbf{V}_{12}\, \Delta p_1(e_1) = \mathbf{j}_2(e_1) \tag{17a}$$

$$\mathbf{j}_2(e_1) - \mathbf{V}_{21}\, \Delta p_2(e_1) = \mathbf{j}_1(e_1) \tag{17b}$$

By assuming that $V_{12}$ and $V_{21}$ are equal, we obtain:

$$\Delta p_1(e_1) = \Delta p_2(e_1) \tag{18}$$

*interface 2 ($z = e_2$):* The boundary condition at interface 2 is similar to that at interface 1:

$$\mathbf{j}_2(e_2) - \mathbf{V}_{23}\, \Delta p_2(e_2) = \mathbf{j}_3(e_2) \tag{19a}$$

$$\mathbf{j}_3(e_2) - \mathbf{V}_{32}\, \Delta p_3(e_2) = \mathbf{j}_2(e_2) \tag{19b}$$

where $\mathbf{j}_2(e_2)$ and $\mathbf{j}_3(e_2)$ are the current densities in layer 2 and in layer 3, respectively. $\mathbf{j}_2(e_2)$ is a pure drift current density, whereas $\mathbf{j}_3(e_2)$ is a pure diffusive current density. $\Delta p_3(e_2)$ and $\Delta p_2(e_2)$ are the minority carrier densities at interface 2.

By assuming that $V_{23}$ is equal to $V_{32}$, similarly to relation (18) we obtain:

$$\Delta p_3(e_2) = \Delta p_2(e_2) \tag{20}$$

Equation (19a) can therefore be written as:

$$(\mu E - V_{23})\,\Delta p_3(e_2) = j_3(e_2) = -D_3 \left.\frac{\mathrm{d}\,\Delta p_3(z)}{\mathrm{d}z}\right|_{e_2} \tag{21}$$

The current density $j_2(e_2)$ at interface 2 is related to $j_2(e_1)$ at interface 1:

$$j_2(e_2) = j_2(e_1) + GE \tag{22}$$

where $GE$ is the total minority carrier generation, by unit time, in the second layer, by the electron beam:

$$GE = \int_{e_1}^{e_2} g(z)\,\mathrm{d}z \tag{23}$$

Relation (22) can also be expressed as a function of the electrical field $E$ in the second layer and of the carrier mobility $\mu$:

$$\Delta p_2(e_2)\,\mu\,E = \Delta p_2(e_1)\,\mu\,E + GE \tag{24}$$

In order to simplify the boundary conditions, we have assumed, in relation (24), that the value of the electrical field is constant in the second layer.

A new relation which takes into account the participation of the three layers is obtained from relations (17) to (24):

$$j_1(e_1) - (V_{12} + V_{23})\,\Delta p_1(e_1) + GE\left(1 - \frac{V_{23}}{\mu E}\right) = j_3(e_2) \tag{25}$$

with $j_1$ and $j_3$ given by relations (6) and (13).

*z infinite:* The minority carrier density $\Delta p_3(z)$ in the substrate is a nil when $z$ is infinite. Therefore, the constant $A_3$ in expression (14) is equal to zero. The coefficients $A_1$, $B_1$ and $B_3$ (Eqs. (8) and (14) are calculated by solving equations (16), (21) and (25). Their values are:

$$B_3 = \frac{\frac{I_3}{2}\left(1 + (\mu E - V_{23})\cdot\frac{L_3}{D_3} + 1\right)}{(D_3/L_3 + V_{23} - \mu E)} \exp\left(\frac{e_2}{L_3}\right) \tag{26}$$

with

$$I_3 = \int_{e_2}^{\infty} \exp\left(\frac{e_2 - z'}{L_3}\right) g(z')\,\mathrm{d}z' \tag{27}$$

$$A_1 = \frac{\alpha(D_1/L_1 + V_0) + \beta(D_1/L_1 - (V_{12} + V_{23}))\exp(-e_1/L_1)}{\Delta}$$

$$B_1 = \frac{\alpha(D_1/L_1 - V_0) + \beta(D_1/L_1 + (V_{12} + V_{23}))\exp(e_1/L_1)}{\Delta}$$

where

$$\Delta = (D_1/L_1 - V_0)\,.\,(D_1/L_1 - (V_{12} + V_{23}))\exp(-e_1/L_1) - (D_1/L_1 + V_0)\,.\,(D_1/L_1 + (V_{12} + V_{23}))\exp(e_1/L_1) \tag{28}$$

$$\beta = \left(\frac{L_1 V_0}{D_1} - 1\right)\frac{I_1}{2} \tag{29}$$

$$\alpha = \frac{I_2}{2}\left(\frac{V_{12} + V_{23}}{D_1/L_1} - 1\right) - \frac{I_3}{2} - GE\left(1 - \frac{V_{23}}{\mu E}\right) + \frac{D_3}{L_3}B_3 \exp\left(-\frac{e_2}{L_3}\right) \tag{30}$$

and

$$I_1 = \int_0^{e_1} \exp(-\frac{z'}{L_1})g(z')\mathrm{d}z' \tag{31a}$$

$$I_2 = \int_{e_1}^{e_2} \exp\left(-\frac{e_1 - z'}{L_1}\right) g\,(z')\,\mathrm{d}z' \tag{31b}$$

We have used in our calculation the depth-dose function $g(z)$ obtained from the three-dimensional generation function $g(\mathbf{r})$ derived by Akamatsu *et al.* [7] from Monte-Carlo simulations:

$$g(z) = a\left(1.1 + 7.13\frac{z}{\left(\frac{r_1}{3}\right)}\right)\pi\left(\sigma_1^2 \exp\left(-\frac{z^2}{\sigma_1^2}\right) + 3.4\,\tau_1^2 \exp\left(-\frac{z^2}{\sigma_2^2}\right) + 96\,\tau_2^2 \exp\left(-\frac{z^2}{\sigma_3^2}\right)\right) \tag{32}$$

$a$ is a normalisation factor, and

$$\sigma_1^2 = 2\left(\frac{r_1}{3}\right)^2 \qquad \sigma_2^2 = 2\left(\frac{r_1}{6}\right)^2 \qquad \sigma_3^2 = 2\left(\frac{r_1}{12}\right)^2$$
$$\tau_1^2 = 2\left(\frac{r_1}{9}\right)^2 \qquad \tau_2^2 = 2\left(\frac{r_1}{27}\right)^2$$

where $r_1$ is the penetration depth of the incident electrons. It is given by the Gruen range:

$$r_1 = \frac{4.57\,E_0^{1.75}}{100\,\rho}$$

where $\rho$ is the density.

## 3. Numerical results

$I_{CL}$ *versus* $E_0$ curves have been calculated as a function of minority carrier diffusion length and optical absorption coefficient of the first layer, of surface/interfaces recombination velocities and of the minority carrier diffusion length of the substrate. The top and buffer layers are 2 $\mu$m and 1 $\mu$m thick respectively. The influence of the thicknesses of these two layers have also been investigated. Calculations have shown that, in most cases, the curves exhibit a maximum, the position of which is called $E_{0m}$ in the following. $E_{0m}$ is located in the range 5 to 40 kV which is experimentally accessible.

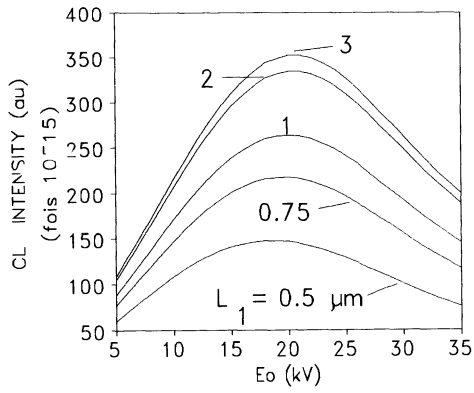


Fig. 2. — Theoretical $I_{CL} = f(E_0)$ curves. The first layer is such that $e_1 = 2$ µm, $N_{D_1} = 2 \times 10^{18}/cm^3$; the second layer is 1 µm thick and of p type. Influence of the minority carrier diffusion length $L_1$ in the first layer. The simulations have been made for $V_0 = V_1 = V_2 = 10^6$ cm/s, $\alpha = 10^4$ cm$^{-1}$, $L_3 = 1$ µm. The minority carrier mobility $\mu$ is equal to 180 cm$^2$/Vs. $T = 300$ K. The CL intensity increases with $L_1$ and the position of the maximum is shifted towards high beam voltages.

**3.1** INFLUENCE OF THE DIFFUSION LENGTH OF THE UPPERMOST LAYER — Figure 2 shows typical CL intensity curves as a function of the accelerating beam voltage $E_0$. The curves, plotted for surface and interfaces recombination rates $V_0$, $V_1$ and $V_2$ of $10^6$ cm/s, are displayed for an optical absorption coefficient $\alpha$ of $10^4$ cm$^{-1}$.

First of all, it has to be noticed that the value taken by $L_1$ influences essentially the position of the maximum, which occurs at a higher beam voltage when $L_1$ increases. Above a certain value of $L_1$, $E_{0m}$ remains the same when all the other parameters are kept constant. In the structure investigated, where the doping level of the uppermost layer is equal to $2 \times 10^{18}/cm^3$, this occurs when the ratio $e_1/L_1$ becomes smaller than 2.

The CL intensity increases with $L_1$; the increase gets smaller when the diffusion length gets larger, as it can be seen in figure 2 where the curves drawn for $L_1 = 2$ µm and for $L_1 = 3$ µm are quite close to each other.

**3.2** INFLUENCE OF SURFACE AND INTERFACES RECOMBINATION VELOCITIES. — The CL intensity curves in figure 3 are plotted for an optical absorption coefficient $\alpha$ of $10^4$ cm$^{-1}$, and those of figures 4 and 5 for $\alpha$ equal to $5 \times 10^3$ cm$^{-1}$.

**3.2.1** *Surface recombination rate* — The presence of the maximum of the CL intensity curve depends on the value of the surface recombination rate as illustrated in figure 3. The curves exhibit a maximum in the 5 to 35 kV range only when $V_0$ is larger than $10^3$ cm/s, whatever is the diffusion length (Figs. 3a and 3d) and whatever are the interfaces recombination rates $V_1$ and $V_2$ (Figs. 3a, 3b and 3c). The low beam voltage part of the curve is the most dependent on $V_0$. The increase of the slope is quite strong when $V_0$ increases from $10^5$ to $10^6$ cm/s.

An increase of $V_0$ always leads to an increase of $E_{0m}$. The value of $E_{0m}$ depends on $V_1$ and $V_2$ (Figs. 3a, 3b and 3c) as well as on $L_1$ (Figs. 3a and 3d). For $V_1 = V_2 = 10^3$ cm/s, the maximum of the CL intensity is not very much pronounced (Fig. 3b). Finally, let us notice that the curves calculated for $V_1 = 10^6$ cm/s and $V_2 = 10^3$ cm/s (Fig. 3c) are identical to those drawn for $V_1 = 10^3$ cm/s and $V_2 = 10^6$ cm/s. Therefore, we have not drawn the curves corresponding to this last set of parameters.

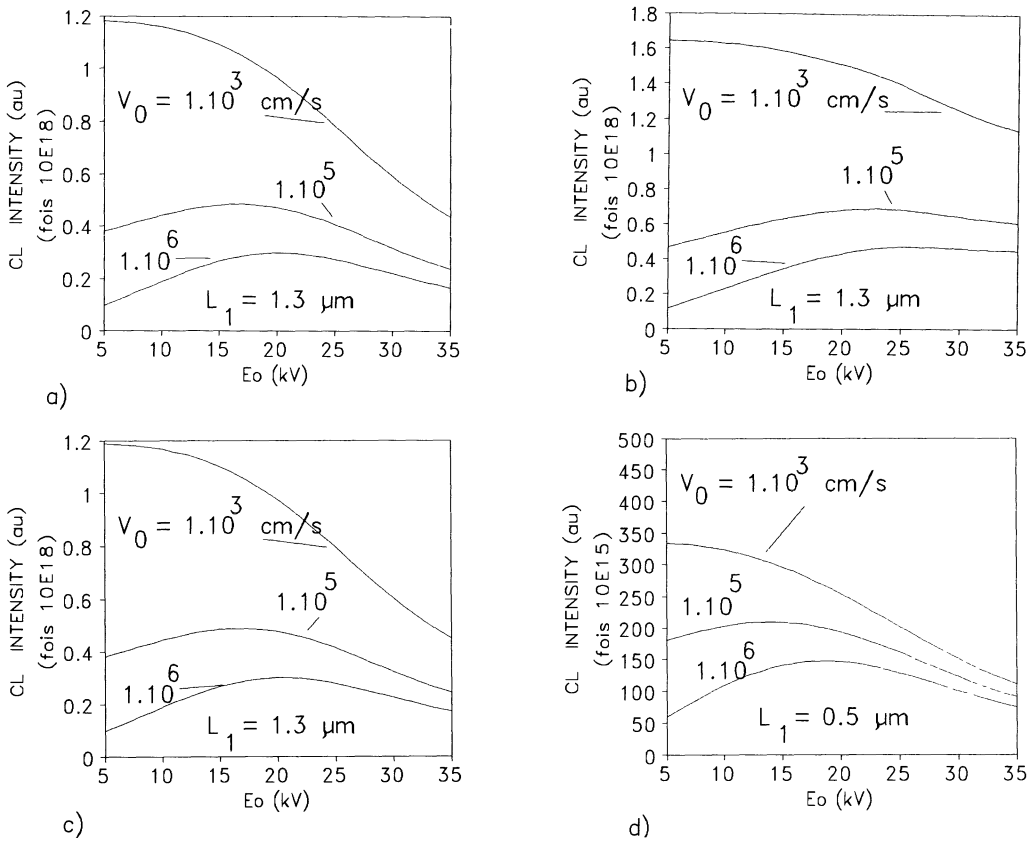


Fig. 3. — Influence of the surface recombination rate $V_0$ on theoretical CL curves for the structure in figure 1. $N_{D_1}$, $\alpha$, $e_1$, $e_2$ and are as in figure 2. When $V_0$ is as low as $10^3$ cm/s, the curve exhibits no maximum. When $V_0$ increases, the maximum moves towards high beam voltages and the slope of the curve before the maximum increases. a) $L_1 = 1.3\ \mu$m; $V_1 = V_2 = 10^6$ cm/s; b) $L_1 = 1.3\ \mu$m; $V_1 = V_2 = 10^3$ cm/s; c) $L_1 = 1.3\ \mu$m; $V_1 = 10^3$ cm/s and $V_2 = 10^6$ cm/s; the same curve is obtained for $V_1 = 10^6$ cm/s and $V_2 = 10^3$ cm/s; d) $L_1 = 0.5\ \mu$m; $V_1 = V_2 = 10^6$ cm/s.

**3.2.2** *First interface recombination rate* — The influence of the first interface recombination rate $V_1$ is shown in figure 4. An increase of $V_1$ leads to a shift of $E_{0m}$ towards low beam voltages and to a decrease of the CL intensity which is more important after $E_{0m}$, only in the case where $V_2$ is as low as $10^3$ cm/s (Fig. 4a). The slope of the curve calculated in the case where $V_1$ and $V_2$ are equal to $10^3$ cm/s is very small and the CL intensity seems to 'saturate' for beam voltages higher than 29 kV (Fig. 4a). The influence of the first interface recombination rate decreases when $V_2$ increases and becomes negligible when $V_2$ is a high as $10^6$ cm/s (Fig. 4b).

**3.2.3** *Second interface recombination rate* — It can be seen in figure 5 that the influence of $V_2$ on the CL curves is similar to that of $V_1$: as a matter of fact, the curves in figure 4a and 5a are identical, as the curves in figure 4b and figure 5b. This means that the recombination of carriers at the first interface is equivalent to that at the second interface; this is consistent with the fact that the two interfaces are separated by a depleted region (Fig. 1).

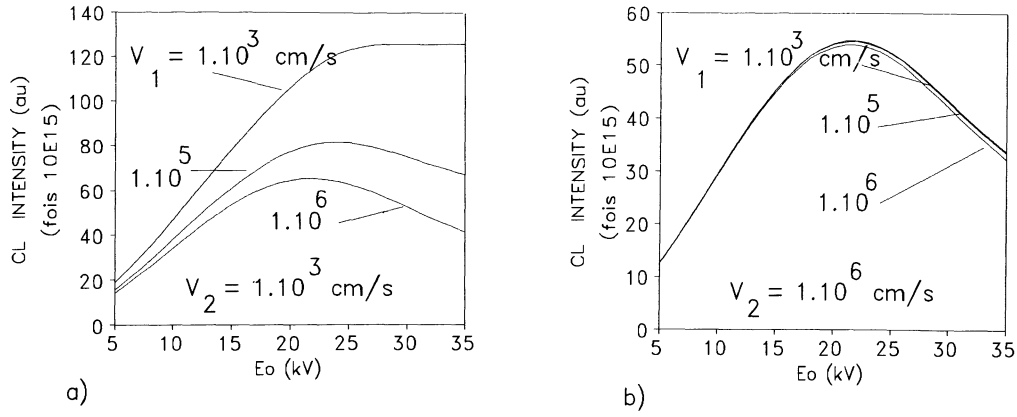


Fig. 4. — Influence of the interface recombination rate $V_1$ on theoretical CL curves for the structure in figure 1. $N_{D_1} = 4 \times 10^{17}/cm^3$, $\alpha = 5 \times 10^3\ cm^{-1}$, $L_1 = 1.5\ \mu m$, $L_3 = 1\ \mu m$, $V_0 = 3 \times 10^6 cm/s$; the values of $e_1$, $e_2$ and $\mu$ are as in figure 2. When $V_1$ is as low as $10^3$ cm/s, the curve exhibits no maximum. When $V_1$ increases, the maximum is shifted towards low beam voltages and the slope of the curve after the maximum increases. a) $V_2 = 10^3$ cm/s; b) $V_2 = 10^6$ cm/s.

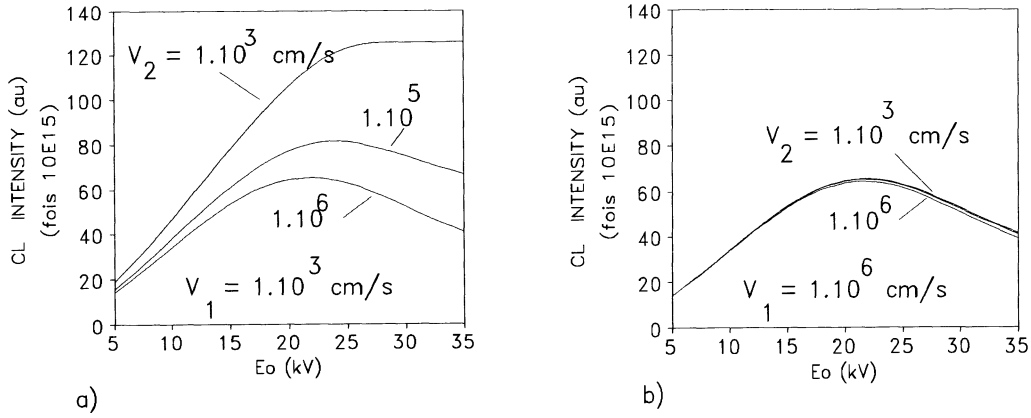


Fig. 5. — Influence of the interface recombination rate $V_2$ on theoretical CL curves for the structure in figure 1. The values of $N_{D_1}$, $\alpha$, $L_1$, $L_3$, $V_0$, $e_1$, $e_2$ and $\mu$ are as in figure 4. When $V_2$ is as low as $10^3$ cm/s, the curve exhibits no maximum. When $V_2$ increases, the maximum is shifted towards low beam voltages and the slope of the curve after the maximum increases. a) $V_1 = 10^3$ cm/s; b) $V_1 = 10^6$ cm/s. The curves in figures 5a and 5b are identical to those in figures 4a and 4b respectively. This means that the values of $V_1$ and $V_2$ cannot be separetely determined.

**3.3** INFLUENCE OF THE OPTICAL ABSORPTION COEFFICIENT — An increase of the optical absorption coefficient $\alpha$ leads to a decrease of the CL intensity (Fig. 6). The resulting shift of $E_{0m}$ towards low beam voltages is a little larger when $L_1$ is smaller. For instance, $E_{0m}$ is shifted from 22 to 20 kV for $L_1 = 1\ \mu m$ (Fig. 6a) and from 22 to 19 kV for $L_1 = 0.5\ \mu m$ (Fig. 6b) when $\alpha$ varies from $10^3$ to $10^4\ cm^{-1}$. The influence of $\alpha$ on the CL intensity is higher at beam voltages equal or higher than $E_{0m}$.

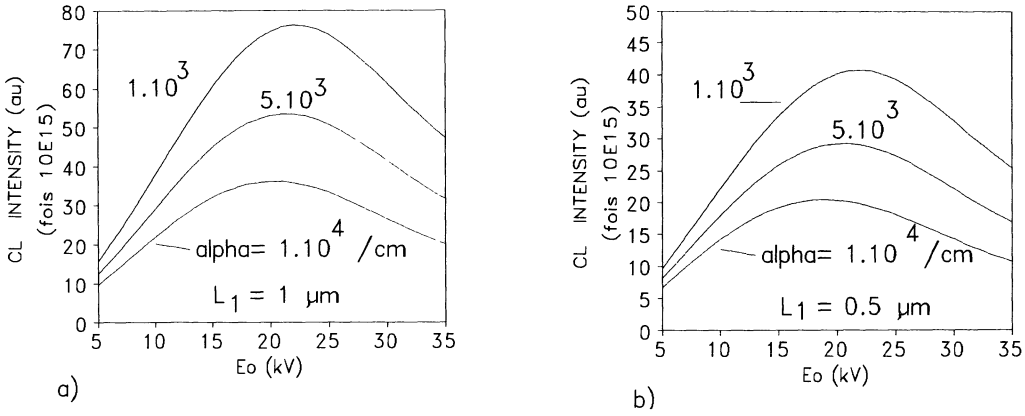


Fig. 6. — Influence of the optical absorption coefficient on theoretical CL curves. $N_{D_1}$, $L_3$, $V_0$, $e_1$, $e_2$ and $\mu$ are the same as in figure 4. a) $L_1 = 1$ µm; b) $L_2 = 0.5$ µm. When $\alpha$ increases, the maximum moves towards low beam voltages and the CL intensity decreases.

**3.4** INFLUENCE OF THE THICKNESS OF THE EPILAYERS — The curves in figures 7 and 8 have been calculated for $L_1 = 1.5$ µm, $L_3 = 1$ µm, $V_0 = 3 \times 10^6$ cm/s and $\alpha = 5 \times 10^3$ cm$^{-1}$.

**3.4.1** *Thickness of the uppermost layer* — The CL intensity increases with the thickness $e_1$ of the uppermost layer, whatever are the interface recombination rates $V_1$ and $V_2$ (Fig. 7). The shape of the CL curve is strongly dependent on the values taken by $V_1$ and $V_2$: for low values of $e_1$ such as 0.5 and 1 µm for instance, the CL curve exhibits two maxima when $V_1 = V_2 = 10^3$ cm/s (Fig. 7a) and one maximum when either $V_1$ or $V_2$ is equal to $10^6$ cm/s (Fig. 7b). The value of $E_{0m}$ increases with $e_1$ whatever are $V_1$ and $V_2$.

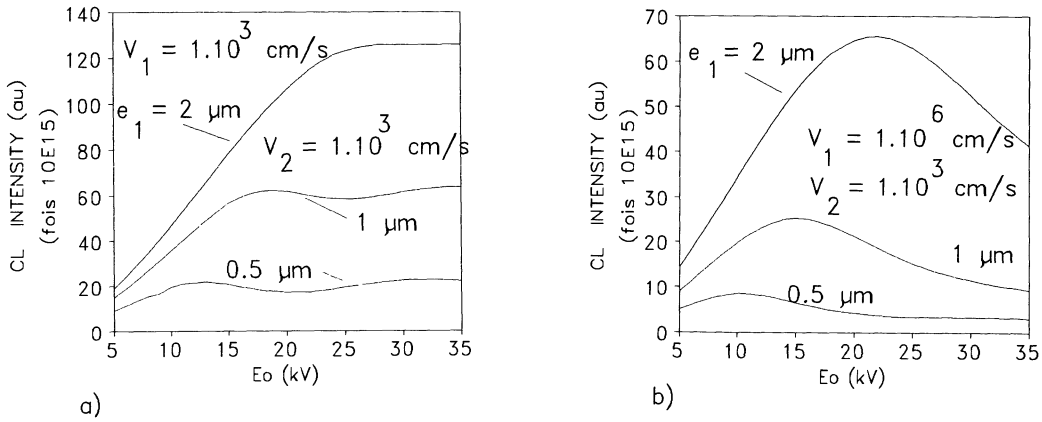


Fig. 7. — Influence of the thickness of the uppermost layer on theoretical CL curves. $N_{D_1}$, $\alpha$, $L_1$, $L_3$, $V_0$, $e_2$ and $\mu$ are the same as in figure 4. a) $V_1 = V_2 = 10^3$ cm/s; b) $V_1 = 10^6$ cm/s, $V_2 = 10^3$ cm/s. When $e_1$ increases, the maximum moves towards high beam voltages and the CL intensity increases, whatever are the values of $V_1$ and $V_2$. Notice, in figure a, the appearance of a second maximum when $e_1$ is equal to 0.5 µm.

3.4.2 *Thickness of the buffer layer* — The CL curves displayed in figure 8 show the infuence of the thickness $e_2$ of the second layer. When the interfaces recombination rates $V_1$ and $V_2$ are equal to $10^3$ cm/s, the CL intensity decreases when $e_2$ increases (Fig. 8a). Futhermore, the CL curves exhibit one maximum for low values of $e_2$, and two maxima for larger values of $e_2$.

The influence of $e_2$ is rather small when either $V_1$ or $V_2$ or both are equal to $10^6$ cm/s (Figs. 8b, 8c, 8d). In that cases, the maximum of the CL intensity occurs at the same beam voltage, and the value of the maximum of CL is a little smaller in case d).

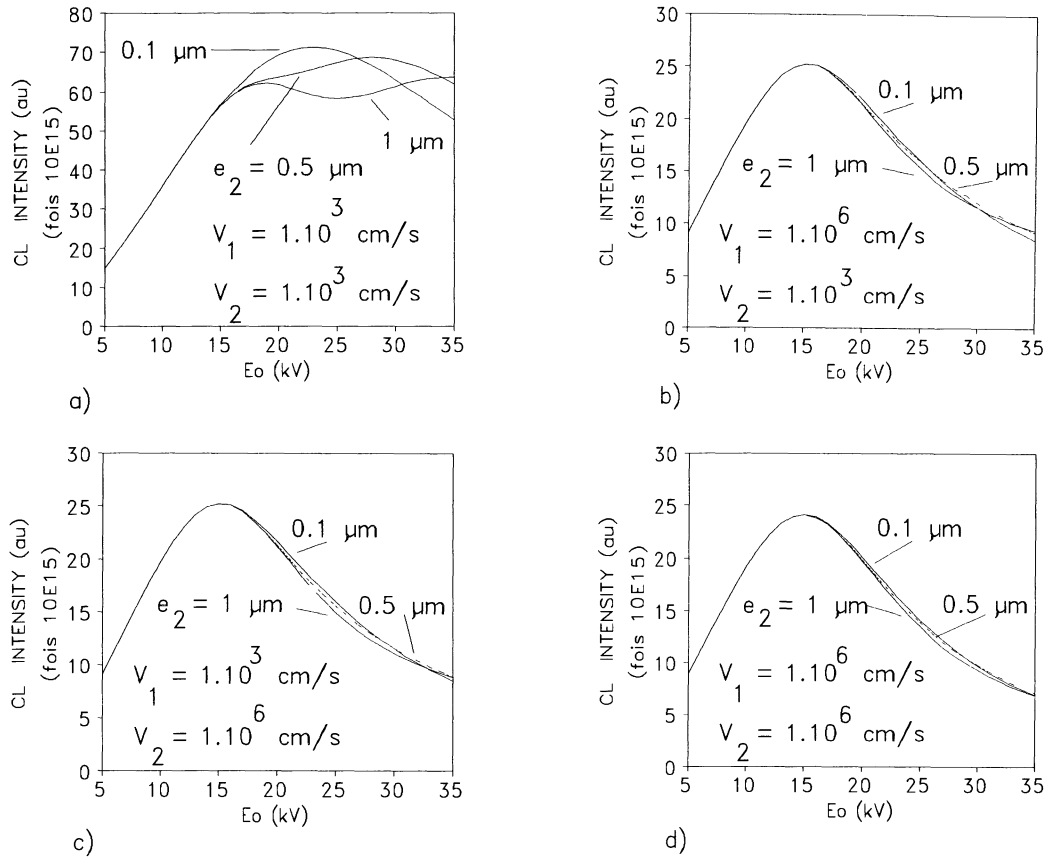


Fig. 8. — Influence of the thickness of the buffer layer on theoretical CL curves. $N_{D_1}$, $\alpha$, $L_1$, $L_3$, $V_0$ and $\mu$ are the same as in figure 4. $e_1 = 1$ $\mu$m. a) $V_1 = V_2 = 10^3$ cm/s; b) $V_1 = 10^6$ cm/s,$V_2 = 10^3$cm/s; c) $V_1 = 10^3$ cm/s, $V_2 = 10^6$ cm/s; d) $V_1 = 10^6$ cm/s, $V_2 = 10^6$ cm/s. When $e_2$ increases, the maximum moves towards high beam voltages and the CL intensity decreases. Notice, in figure 8a, the appearance of a second maximum when $e_2$ is equal to 1 $\mu$m.

3.5 INFLUENCE OF THE DIFFUSION LENGTH $L_3$ OF THE SUBSTRATE — The value of the diffusion length $L_3$ influences the CL curves when the thicknesses of the uppermost and buffer are indeed small enough to allow the electron beam to penetrate into the substrate. An increase of $L_3$ leads to an increase of the CL intensity at high beam voltage (Fig. 9). The increase is higher when the interface recombination velocities $V_1$ and $V_2$ are smaller; in that case, the CL curve can even exhibit a second maximum (Fig. 9a).

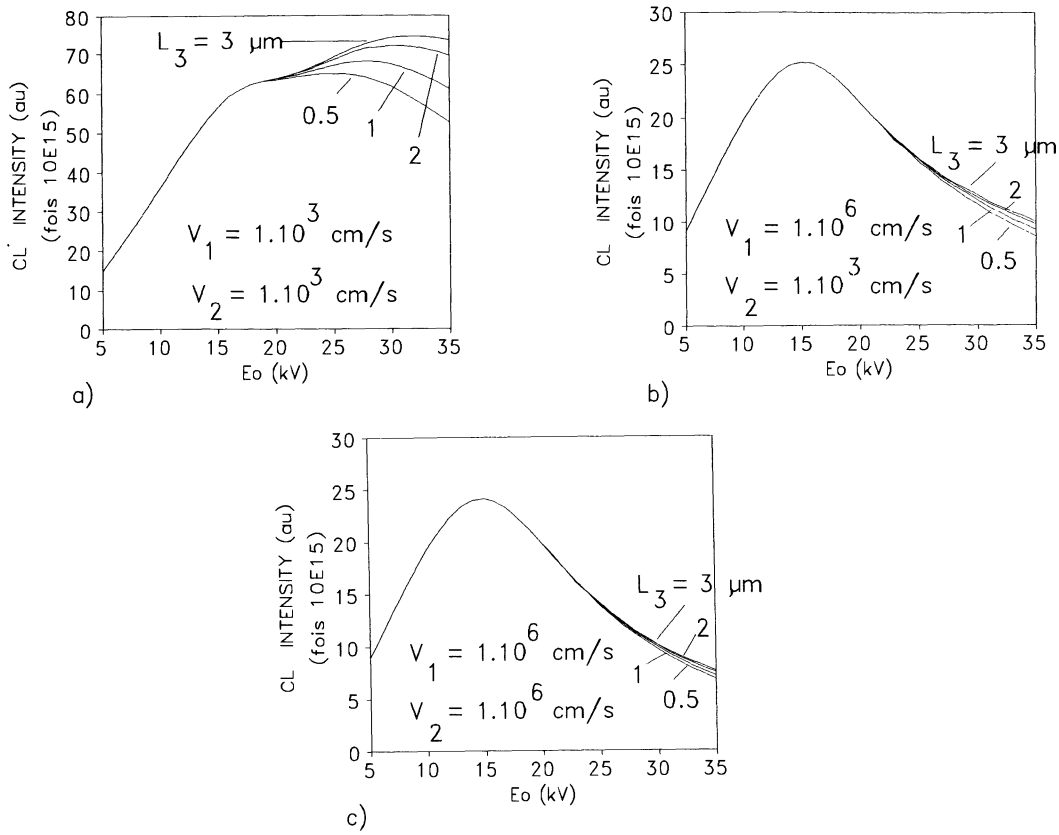


Fig. 9. — Influence of the diffusion length of the substrate on theoretical CL curves. $N_{D_1}$, $\alpha$, $L_1$, $V_0$ and $\mu$ are the same as in figure 4. $e_1 = 1\ \mu m$; $e_2 = 0.5\ \mu m$. a) $V_1 = V_2 = 10^3$ cm/s; b) $V_1 = 10^6$ cm/s, $V_2 = 10^3$ cm/s; or $V_1 = 10^6$ cm/s, $V_2 = 10^3$ cm/s; c) $V_1 = 10^6$ cm/s, $V_2 = 10^6$ cm/s. In case b), when $L_3$ increases, a second maximum appears on the CL curve which moves towards high beam voltages and the CL intensity increases.

**3.6** DISCUSSION OF THE THEORETICAL CL INTENSITY CURVES — In table I are collected all the effects of the various parameters on the CL intensity, on the presence and position of $E_{0m}$, as well as on the slopes of the curves.

The occurence of the maximum is mainly dependent on the surface recombination velocity $V_0$ (Fig. 3) and, for a ratio $e_1/L_1$ smaller than 2, on the first and second interface recombination rates (Figs. 4a and 5a). For low values of $V_0$ the CL intensity decreases when $E_0$ increases, whereas for low values of $V_1$ and / or $V_2$ it increases with $E_0$. In real cases where $V_0$ is in the range $10^5$ (InP for instance) to few $10^6$ (GaAs) cm/s, and for thicknesses of the uppermost layer $e_1$ such that $e_1/L_1 < 2$, the CL intensity curve exhibits a maximum if $V_1$ and $V_2$ are not as low as $10^3$ cm/s.

The position of $E_{0m}$ is strongly related to $L_1$ (Fig. 2), $V_0$ (Fig. 3), $V_1$ (Fig. 4), $V_2$ (Fig. 5), $\alpha$ (Fig. 6); in structures with thin uppermost and buffer layers, the diffusion length $L_3$ in the substrate does influence $E_{0m}$.

A small variation of the doping level will lead to a small change of the CL intensity (cf. Eq. (6)) and of the slope of the curve due to a variation in the minority carrier diffusion length (Fig. 2).

This method of characterisation of epitaxial layers, at a local scale, alloys one to assign different

Table I. — *Influence of the different parameters on the CL intensity recorded as a function of electron beam voltage.*

| parameters influence | $L_1$ | $L_3$ | $V_0$ | $V_1$ | $V_2$ | $\alpha$ | $e_1$ | $e_1 - e_2$ |
|---|---|---|---|---|---|---|---|---|
| presence of a maximum | no | yes(*) | yes | yes | yes | no | yes(*) | yes(*) |
| position of the maximum | strong (→) | no | strong (→) | strong (←) | strong (←) | strong (←) | yes(**) | yes(**) |
| 1st part of the curve | yes | no | strong | weak | weak | no | strong | no |
| 2nd part of the curve | yes | yes | weak | strong | strong | no | strong | yes |

(*) a second maximum can occur in the case $V_1 = V_2 = 10^3$ cm/s
(**) if $V_1 = V_2 = 10^3$ cm/s

sets of parameters ($L_1$, $V_0$, $V_1$, $V_2$, $\alpha$) to the first layer, if none of them is known before undertaking the experiments. It has to be kept in mind that, as a result of the energy bands of the homostructure (Fig. 1), $V_1$ and $V_2$ cannot be identified separately (Figs. 4 and 5). In fact a lower limit of $L_1$, $V_0$, $V_1$ and $V_2$ values can be unambiguously determined, as well as an upper limit of the value of $\alpha$. Thus, as shown in the next section, information on the quality of the uppermost layer can be easily obtained by this technique.

## 4. Limits of the technique: experimental characterisation of GaAs homojunctions.

To determine the limits of the method, we have studied GaAs homojunctions such as those described previously, with two silicon doping levels of the uppermost layer: $4 \times 10^{17}/\text{cm}^3$ and $2 \times 10^{18}/\text{cm}^3$. ($e_1 = 2\ \mu$m, $e_2 - e_1 = 1\ \mu$m). The specimens were grown by MBE at 580 °C. The polychromatic CL intensity has been recorded for variation steps of 2 kV of the accelerating voltage. Close to the maximum, the step was reduced to 1 kV. The experiments have been carried out in a Stereoscan 250 MK3 Cambridge scanning microscope, equipped with an Oxford CL attachment. The center and the edges of the 2 inches wafers have been characterised. The luminescence intensity has been found, in all specimens, quite homogeneous. The results presented in the following have been averaged over about three or four measurements.

- $N_D = 4 \times 10^{17}/\text{cm}^3$

In figure 10 is shown the best fit obtained for the CL intensity curve recorded on the first specimen. It has been chosen among four other ones for which the position of $E_{0m}$ is located at 22 kV:

a) $L_1 \geq 1\ \mu$m, $L_3 = 1\ \mu$m, $V_0 = 3 \times 10^6$ cm/s,
$V_1 \geq 10^3$ cm/s, $V_2 = 10^6$ cm/s, $\alpha = 10^3\ \text{cm}^{-1}$.

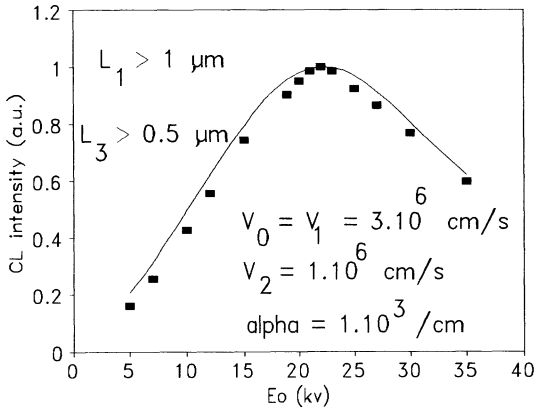


Fig. 10. — Fit of a polychromatic CL intensity curve recorded at 300 K on a Si doped GaAs ($n = 4 \times 10^{17}/\text{cm}^3$; 2 $\mu$m thick)/GaAs ($N_A = 10^{15}/\text{cm}^3$; 1 $\mu$m thick)/Si GaAs homojunction. The maximum of the curve occurs at 22 kV. The parameters of the structure are: $L_1 > 1$ $\mu$m, $L_3 > 0.5$ $\mu$m, $V_0 = V_1 = 10^6$ cm/s, $V_2 = 10^6$ cm/s, $\alpha = 10^3$ cm$^{-1}$.

b) $L_1 \geq 1$ $\mu$m, $L_3 = 1$ $\mu$m, $V_0 = 3 \times 10^6$ cm/s,
$V_1 \geq 10^3$ cm/s, $V_2 = 10^6$ cm/s, $\alpha = 5 \times 10^3$ cm$^{-1}$.

c) $L_1 \geq 1.3$ $\mu$m, $L_3 = 1$ $\mu$m, $V_0 = 3 \times 10^6$ cm/s,
$V_1 \geq 10^5$ cm/s, $V_2 = 10^6$ cm/s, $\alpha = 5 \times 10^3$ cm$^{-1}$.

d) $L_1 \geq 0.5$ $\mu$m, $L_3 = 1$ $\mu$m, $V_0 > = 1 \times 10^6$ cm/s,
$V_1 \geq 10^6$ cm/s, $V_2 = 10^6$ cm/s, $\alpha = 10^3$ cm$^{-1}$.

The range of suitable surface recombination velocities is not as large $\left(V_0 > 10^6 \text{ cm/s}\right)$ as that of suitable interface recombination velocities $(V_1 \geq 10^3 \text{ cm/s})$ and diffusion lengths $(L_1 >= 0.5$ $\mu$m$)$.

The difference between the experimental and the theoretical curves at low and high beam voltages could result from the presence of small residual space charge regions close to the free surface and to the first interface, which have not been taken into account in our model. Their presence could result from the fact that the energy bands have not been completely flattened by the electron beam injection. The minority carrier diffusion length and the recombination surface velocity values correspond to those generally found in GaAs of good quality where recombination is not controlled by deep levels [8-10]. The value given for $L_3$ is quite meaningless since it cannot be determined accurately. This results from the large thickness of the uppermost and buffer layers with respect to the penetration depth of the 35 kV incident electrons and from the high value of the interfaces recombination velocities (cf. Fig. 9).

• $N_D = 2 \times 10^{18}/\text{cm}^3$

The maximum of the CL curve is located at 21 kV (Fig. 11), which corresponds to:

a) $L_1 \geq 1$ $\mu$m, $L_3 = 1$ $\mu$m, $V_0 = 3 \times 10^6$ cm/s,
$V_1 = 10^6$ cm/s, $V_2 = 10^6$ cm/s, $\alpha = 5 \times 10^3$ cm$^{-1}$.

b) $L_1 \geq 1$ $\mu$m, $L_3 = 1$ $\mu$m, $V_0 = 3 \times 10^6$ cm/s,
$V_1 \geq 10^6$ cm/s, $V_2 >= 10^6$ cm/s, $\alpha = 5 \times 10^3$ cm$^{-1}$.

c) $L_1 \geq 1.3\ \mu m$, $L_3 = 1\ \mu m$, $V_0 = 3 \times 10^6$ cm/s, .
$V_1 \geq 10^6$ cm/s, $V_2 = 10^6$ cm/s, $\alpha >= 5 \times 10^3$ cm$^{-1}$.

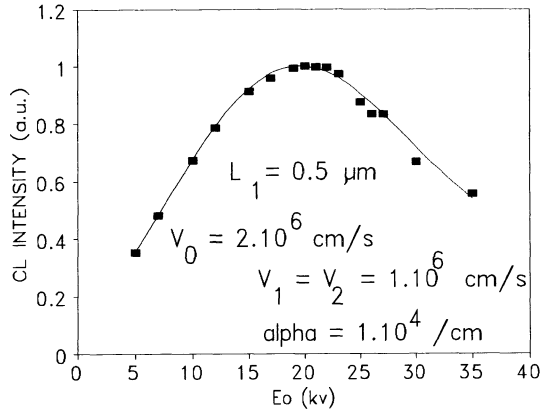


Fig. 11. — Fit of a polychromatic CL intensity curve recorded at 300 K on the same structure as in figure 10, but the silicon doping level of the uppermost layer is equal to $2 \times 10^{18}$/cm$^3$. The maximum of the CL intensity is in the range 20 – 22 kV. The parameters of the structure are: $L_1 = 0.5\ \mu m$, $L_3 > 0.5\ \mu m$, $V_0 = 2 \times 10^6$ cm/s, $V_1 = V_2 = 10^6$ cm/s, $\alpha = 10^4$ cm$^{-1}$.

The theoretical curves a) b) and c) do not fit well the experimental curve as a whole. The shape of the computed curve shown in figure 11 is the only one to be in good agreement with that recorded experimentally. Its maximum is located at 19 kV and not at 21 kV as that of the experimental curve. This result from the fact that the experimental maximum is not very much marked and that the CL intensity is in fact more or less constant between 19 and 22 kV. This illustrates that the determination of $L_1$ requires a fit of the whole curve and not to rely only on the position of the maximum.

The minority carrier diffusion length decreases and the lower limit of the optical absorption coefficient increases when the doping level goes up from $4 \times 10^{17}$/cm$^3$ ($L_1 > 1\ \mu m$; $\alpha = 5 \times 10^3$ cm$^{-1}$) to $2 \times 10^{18}$/cm$^3$ ($L_1 = 0.5\ \mu m$; $\alpha = 10^4$ cm$^{-1}$). The value of the absorption coefficient is an averaged one since polychromatric CL has been recorded in a wavelength range where its variation is very steep. In order to avoid light absorption by the specimen, experiments could be performed in the infra-red.

## 5. Conclusions.

We have undertaken a CL characterisation of silicon doped GaAs epitaxial layers grown by MBE. A model describing the variation of the CL intensity with the electron beam voltage has been developed in order to determine parameters such as the minority carrier diffusion length in the uppermost layer and the surface and interfaces recombination velocities. The band structure of the specimen has been taken into account in order to write well adapted boundary conditions. It has been shown that the optical absorption coefficient has also to be taken into account. The minority carrier diffusion length, whose value gives information on the quality of the layer, cannot be determined solely from the position of $E_{0m}$ of the CL curve. A fit of the whole curve in the range

5 to at least 35 kV is necessary. This has been applied to the characterisation of 2 microns thick GaAs layers silicon doped at $4 \times 10^{17}$ and $2 \times 10^{18}/cm^3$. Despite the large number of parameters involved in the CL signal formation, their determination was quite easy. A lower limit of the diffusion length, which was found to decrease when the doping level increases, and an upper limit of the optical absorption coefficient could be given.

When available, one has to take advantage of the CL technique since it gives valuable information on the free surface and interfaces qualities without any specimen preparation. An accurate determination of the minority carrier diffusion length $L_1$, when it is smaller than $(1/\alpha)$, requires another technique such as EBIC for instance. When $L_1$ is greater than $(e_1/2)$, another homostructure with a thicker uppermost layer is necessary. On the opposite, thin uppermost layers can be used to determined the interfaces recombination velocities.

## References

[1] WU C.J. and WITTRY D.B. *J. Appl. Phys.* **49** (1978) 2827.
[2] HERGERT W., RECK P., PASEMANN L., SCHREIBER J., *J. Phys. Stat. Sol (a)* **101** (1987) 611.
[3] HILDEBRANDT S., SCHREIBER J., HERGERT W. and PETROV V.I., *Phys. Stat. Sol. (a)* **110** (1988) 283.
[4] ACHOUR S., *Phil. Mag. Lett.* **59** (1989) 205.
[5] KONNIKOV S.G. *et al., Soviet Phys. Semicond.* **20** (1986) 661.
[6] MARTINS R.B., Thèse d'Université, Orsay, 1991.
[7] AKAMATSU B., HENOC P. and MARTINS R.B., *J. Microsc. Spectrosc. Electron.* **14** (1989) 12a.
[8] TARRICONE L., FRIGERI C., GOMBIA E. and ZANOTTI L., *J. Appl. Phys.* **60** (1986) 1745.
[9] JASTRZEBSKI L., LAGOWSKI J. and GATOS H.C., *Appl. Phys. Lett.* **27** (1975) 537.
[10] HOFFMAN C.A., GERRITSEN H.J. and NURMIKKO A.V., *J. Appl. Phys.* **51** (1980) 1603.